ACS APPLIED MATERIALS & INTERFACES

Research Article

www.acsami.org

Functionalization of Alkyne-Terminated Thermally Hydrocarbonized Porous Silicon Nanoparticles With Targeting Peptides and Antifouling Polymers: Effect on the Human Plasma Protein Adsorption

Chang-Fang Wang,*[,†] Ermei M. Mäkilä,[†,§] Colin Bonduelle,[‡] Jussi Rytkönen,[∥] Janne Raula,[⊥] Sérgio Almeida,[†] Ale Närvänen,[∥] Jarno J. Salonen,[§] Sebastien Lecommandoux,[‡,¶] Jouni T. Hirvonen,[†] and Hélder A. Santos*[,†]

[†]Division of Pharmaceutical Chemistry and Technology, Faculty of Pharmacy, University of Helsinki, FI-00014 Helsinki, Finland

[§]Laboratory of Industrial Physics, Department of Physics and Astronomy, University of Turku, FI-20014 Turku, Finland

[‡]Université de Bordeaux/IPB, ENSCBP, 16 Avenue Pey Berland, 33607, Pessac Cedex, France

[∥]School of Pharmacy, University of Eastern Finland, FI-70211 Kuopio, Finland

[⊥]Department of Applied Physics, Aalto University School of Science, P.O. Box 15100, FIN-00076 Aalto, Espoo, Finland

[¶]CNRS, Laboratoire de Chimie des Polymeres Organiques (UMR5629), 33607 Pessac Cedex, France

Supporting Information

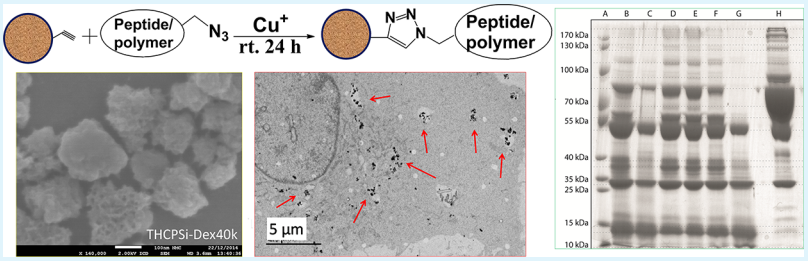

ABSTRACT: Porous silicon (PSi) nanomaterials combine a high drug loading capacity and tunable surface chemistry with various surface modifications to meet the requirements for biomedical applications. In this work, alkyne-terminated thermally hydrocarbonized porous silicon (THCPSi) nanoparticles were fabricated and postmodified using five bioactive molecules (targeting peptides and antifouling polymers) via a single-step click chemistry to modulate the bioactivity of the THCPSi nanoparticles, such as enhancing the cellular uptake and reducing the plasma protein association. The size of the nanoparticles after modification was increased from 176 to 180−220 nm. Dextran 40 kDa modified THCPSi nanoparticles showed the highest stability in aqueous buffer. Both peptide- and polymer-functionalized THCPSi nanoparticles showed an extensive cellular uptake which was dependent on the functionalized moieties presented on the surface of the nanoparticles. The plasma protein adsorption study showed that the surface modification with different peptides or polymers induced different protein association profiles. Dextran 40 kDa functionalized THCPSi nanoparticles presented the least protein association. Overall, these results demonstrate that the "click" conjugation of the biomolecules onto the alkyne-terminated THCPSi nanoparticles is a versatile and simple approach to modulate the surface chemistry, which has high potential for biomedical applications.

KEYWORDS: *surface modification, porous silicon, cell−nanoparticle interaction, click chemistry, protein adsorption*

1. INTRODUCTION

Nanomedicine has been intensively investigated for healthcare applications during the past decades. The aim of nanomedicine is to develop more efficient and low side effect drug delivery systems. Many nanosystems have already shown promising preclinical[1−3] and clinical results.[2,4−6]

Porous silicon (PSi) nanoparticles have a number of unique properties that render them as a potential drug delivery nanovehicle, such as increasing the dissolution rate of poorly water-soluble drugs,[7] high drug loading capacity,[8] and controllable surface structure for further modification to meet the biomedical application requirements.[1,9−12] The native Si−H_x (x = 1−4) terminated PSi surface is highly reactive and prone to spontaneous oxidation in the air.[13] Surface passivation via hydrosilylation, thermal oxidation, thermal carbonization, or thermal hydrocarbonization has been used to stabilize the PSi surface.[8,14] By using different stabilization methods, the hydrophilicity and resistance to degradation of the PSi

Received: November 8, 2014
Accepted: December 25, 2014
Published: December 25, 2014

DOI: 10.1021/am507827n
ACS Appl. Mater. Interfaces 2015, 7, 2006−2015

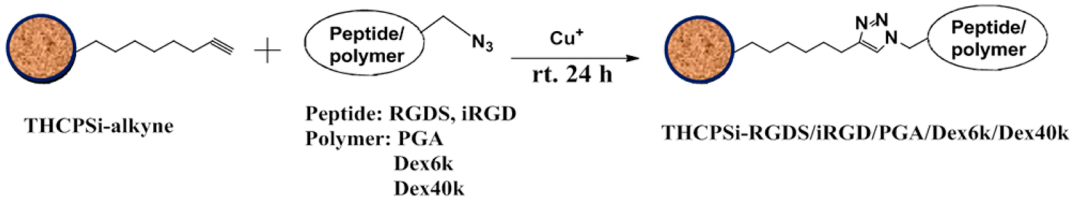

Figure 1. Schematics of the surface modification of THCPSi-alkyne nanoparticles with peptides (RGDS and iRGD), PGA, and dextrans 6 and 40 kDa.

nanomaterials can be tailored.[15] Besides stabilizing the native surface of PSi, chemically reactive moieties can be introduced to PSi nanoparticles surface such as amine[16] and carboxylic acids,[17,18] which can be used for further surface modification. Furthermore, an alkyne terminus has been introduced to the PSi films or substrates by hydrosilylation, which was functionalized with oligoether moieties or antimicrobial peptides via copper-catalyzed azide−alkyne cycloaddition (CuAAC).[19−23] After modification, the PSi films showed improved resistance toward the nonspecific adsorption of proteins.[20,21,23] With chemical surface modifications after the primary stabilization, specific functionalities can be introduced to PSi nanomaterials with the desired properties such as charge, wettability, lipophilicity, and bioactivity.[22,24−27] CuAAC click reaction has been reported as a simple method to couple organic molecules between the azide and alkyne groups in high yields under mild conditions with high selectivity in the presence of a diverse range of other functional groups.[28,29] Both the azide and alkyne groups are almost entirely unreactive to other functional groups such as amines, carboxylic acids, and thiols which are widely present in natural molecules.[30,31] Thus, click chemistry is an interesting approach for the biofunctionalization of nanoparticles by targeting peptides and polymers to the nanoparticles.[24,32]

When the nanoparticles are applied *in vivo* and exposed to the biological fluids, for example the bloodstream, the biomolecules and proteins can adsorb onto the surface of the nanoparticles and develop the so-called "bio−nano interface".[33,34] This protein associated corona can dramatically affect the fate of the nanoparticles *in vivo*. In particular, nanoparticles associated with the complement proteins, immunoglobulins, and fibrinogen proteins can be rapidly recognized by the immune system and induce phagocytosis by the mononuclear phagocyte system (MPS).[35] The surface modification of the nanoparticles to introduce a hydrophilic layer on the nanoparticles can modulate the plasma protein association.[36] For example, poly(ethylene) glycol (PEG) has been incorporated to various nanoparticles to reduce the protein corona.[37−39] However, the surface configuration of PEG does not benefit cellular uptake.[36,38] Cellular uptake of the nanocarrier is an important factor for transporting therapeutic molecules into the targeted cells. It has been reported that hydrophilic dextran shell formed in self-assembling nanoparticles could help to prevent the complement C3 protein activation and fibrinogen adsorption to certain extend depending on the density of the dextran shell.[40] Furthermore, the dextran shelled polymeric nanoparticles presented good cellular uptake.[41]

On the other hand, targeting peptides have also been widely used for the surface modification of nanoparticles to achieve enhanced cellular uptake and *in vivo* targeting drug delivery.[24,42] The protein adsorption profiles of targeting peptides modified nanoparticles is also important regarding the protein corona, because this makes the *in vivo* targeting rather challenge.[43] Poly(glutamic acid) (PGA) is another antifouling and biodegradable hydrophilic polymer that has been widely used in drug delivery applications.[44−46] PGA is a polymer with peptide backbond and has also been reported to present no toxicity[47] and increased the cell uptake of nanocomposites.[48]

Here, alkyne-terminated THCPSi nanoparticles (THCPSi-alkyne) were fabricated for further functionalization by CuAAC. The targeting peptides RGDS (MW 545 Da) and iRGD (MW 1060 Da), PGA (MW 7740 Da), and dextran (MW 6800 Da and 40 kDa) were conjugated to the THCPSi-alkyne nanoparticles to improve the bioactivity of the nanoparticles (Figure 1). The effects of the surface modified nanoparticles on the aqueous stability, cytotoxicity, cellular uptake, and plasma protein adsorption were evaluated.

2. EXPERIMENTAL PROCEDURES

2.1. Materials and Cell Culturing. N-Terminal azidoalanine-functionalized peptides RGDS and iRGD were custom orders from GenicBio (Shanghai, China) based on previous report.[42] γ-Benzyl-L-glutamate-*N*-carboxyanhydride (PBLG-NCA) was purchased from Isochem. Dextran T10 and dextran T40 were purchased from Amersham Biosciences (Orsay, France). All the other chemicals and solvents were purchased from Sigma-Aldrich (USA) with analytical grade and used as received.

Hypoxanthine-aminopterin-thymidine (50× HAT) was purchased from Gibco (Carlsbad, USA). Dulbecco's phosphate buffer saline (10× PBS), Hank's balanced salt solution (10× HBSS), Dulbecco's Modified Eagle's Medium (DMEM), fetal bovine serum (FBS), trypsin (2.5%), sodium pyruvate, nonessential amino acids (100× NEAA), L-glutamine (100×), and penicillin-streptomycin (100×) were purchased from HyClone (Waltham, USA). CellTiter-Glo luminescent cell viability assay kit was purchased from Promega (Madison, USA). Endothelial EA.hy926 (ATCC, USA) cells were incubated in DMEM with high glucose and 2% HAT, while U87 MG (ATCC, USA) brain cells were cultured with DMEM with low glucose. Both cell lines were cultured in 75 cm^2 flasks for further experiments at 37 °C with humidified atmosphere (95%) and 5% CO_2, supplemented by 10% FBS, 1% sodium pyruvate, 1% NEAA, 1% L-glutamine, and 1% penicillin-streptomycin (100 IU/mL).

2.2. Preparation of THCPSi-Alkyne Nanoparticles. Multilayer PSi films were fabricated by electrochemically etching monocrystalline p+-type Si ⟨100⟩ wafers of 0.01−0.02 Ωcm resistivity in a 1:1 (v/v) aqueous hydrofluoric acid (40%)−ethanol electrolyte with a pulsed etching profile as described previously.[49] The obtained free-standing multilayer films were dried and then placed in a quartz tube under N_2 flush at room temperature for at least 30 min. Acetylene (C_2H_2) was then added to the flush at 1:1 (vol) ratio for 15 min at room temperature, followed by inserting the tube in a furnace at 500 °C for another 15 min under continuous N_2/C_2H_2 flush. After removing the quartz tube from the furnace, the obtained THCPSi films were allowed to cool back to room temperature under N_2 flush. Adapting the thermal addition process used previously,[50] the THCPSi films were treated in 10 vol % 1,7-octadiyne−mesitylene solution at 150 °C for 16 h. The films were then wet-milled in a fresh 10 vol % octadiyne−

DOI: 10.1021/am507827n
ACS Appl. Mater. Interfaces 2015, 7, 2006−2015

mesitylene solution into THCPSi-alkyne nanoparticles. The excess chemicals were removed by repeated washing and redispersion into ethanol. The final size selection of the nanoparticles was done by centrifugation.

2.3. Synthesis of the Azide-Functionalized PGA and Dextran. 1-Azido-3-aminopropane and azide functionalized poly(γ-benzyl-L-glutamate) were prepared as described elsewhere (by ^{1}H NMR in chloroform-d ($CDCl_3$) with 15% trifluoroacetic acid (TFA), degree of polymerization (D_p = 55).[44,51,52] Debenzylation of the polypeptide (>95% yield by ^{1}H NMR in DMSO-d^6) was achieved in 90 min. By treatment with hydrogen bromide (HBr) in trifluoroacetic acid (TFA) at room temperature, affording azide functionalized PGA.[52] For all the prepared compounds, the spectroscopic data were in agreement with previously published data.

Dextran T10 (6.5 g, 0.97 mmol) was solubilized in acetate buffer (pH = 5.6), at 2 wt %. 1-Azido-3-aminopropane (6.3 g, 72.9 mmol) was added under magnetic stirring. Then, 4.6 g of $NaCNBH_3$ (72.9 mmol, 75 equiv) were added and the mixture was stirred for 2 days at 30 °C. Subsequently, the mixture was concentrated under vacuum, precipitated in cold methanol, and collected by centrifugation to remove the excess of 1-azido-3-aminopropane and sodium cyanoborohydride. The reaction medium was then dialyzed 4−5 days against Milli-Q water (Spectra/Por6MWCO 50 kDa membrane) to remove the excess of reactants and lyophilized. The obtained yield was 5.9 g (91%). ^{1}H NMR analysis was performed in DMSO-d^6 to verify the full disappearance of the reducing end group anomeric proton peaks. ^{1}H NMR (400 MHz, DMSO, δ, ppm): 4.92 (s broad, 40H, C_4OH), 4.84 (s broad, 40H, C_3OH), 4.70 (s broad, 40H, C_1H_{anom}), 4.49 (s broad, 40H, C_2OH), 3.76 (s broad, 40H, C_6H), 3.53 (s broad, 40H, C_5H), 3.45 (s broad, 40H, C_6H'), 3.22 (s broad, 80H, C_2H + C_4H) (Figure S1). The Fourier transform infrared spectroscopy (FTIR) spectrum (Figure S2) was performed to verify the presence of the N_3 group at the reducing end. The obtained FTIR bands were (cm^{-1}): 3100−3600 (band: 3300), 2920, 2150, 1200−1450 (multiple bands). Size exclusion chromatography (SEC) in water was used to characterize the dextran before (M_n = 6600 g/mol) and after reductive amination (M_n = 6800 g/mol). Azide terminal-functionalized dextran 40 kDa was prepared in a similar way as dextran 6 kDa with the same molarity.

2.4. Surface Modification of THCPSi-Alkyne Nanoparticles by CuAAC. About 2 μmol of each azide-functionalized compounds (RGDS 1.09 mg, iRGD 2.12 mg, dextran 6 kDa 10 mg, and dextran 40 kDa 80 mg) were dissolved in anhydrous DMSO, and PGA (2 μmol, 14 mg) was dissolved in Milli-Q water. Next, 2 mg of the THCPSi-alkyne nanoparticles, 2 μmol copper(II) sulfate pentahydrate, and 20 μmol sodium ascorbate were added to each reaction and kept for stirring at room temperature protected from the light for 24 h. After reaction, the nanoparticles were collected from the reaction mixture by centrifugation (Sorvall RC 5B plus, thermo Fisher Scientific, USA) at 16,100*g* for 3 min and washed with 1 mL of DMSO (the nanoparticles reacted with PGA were washed with ethanol:water, 50:50, vol %), water, and ethanol three times. The modified nanoparticles were resuspended in ethanol for further use.

2.5. Physical Characterization of the Nanoparticles. The specific surface area, pore volume and pore size were determined by N_2 sorption at 77 K using TriStar 3000 (Micromeritics Inc., USA). The specific surface area of the PSi nanoparticles was calculated using the Brunauer−Emmett−Teller theory.[53] The total pore volume was obtained as the total adsorbed amount at a relative pressure p/p_0 = 0.97.

Qualitative analysis of the surface modification was performed by FTIR with a Vertex 70 spectrometer (Bruker Optics, USA) using a horizontal attenuated total reflectance accessory (MIRacle, PIKE Technologies, USA). The spectra were recorded between 4000−650 cm^{-1} with a 4 cm^{-1} resolution. The efficiency of the surface modification was determined by thermogravimetric (TG) measurements (PerkinElmer TGA 7) using a nitrogen flow of 200 mL/min. The samples were heated from 25 to 800 °C.

Elemental analysis (carbon, nitrogen and hydrogen) of the modified nanoparticles were performed on a Vario Micro cube CHN analyzer (Elementar Analysensynstene, GmbH).

The hydrodynamic diameter (Z-average) measured by dynamic light scattering (DLS) and the zeta (ζ)-potential measurements of the nanoparticles were carried out using a Zetasizer Nano ZS (Malvern Instruments, UK) at 25 °C.

High-resolution scanning electron microscopy (HR-SEM) and transmision electron microscopy (TEM) were used to evaluate the morphology of the nanoparticles. HR-SEM images were taken by a SEM (Jeol JSM-7500F, Japan) with a voltage of 10 kV. TEM images were taken by a TEM (Jeol, JEM-1400, Japan) with the voltage of 80 kV.

The stability of the nanoparticle's suspensions in aqueous Hank's balanced salt solution (HBSS) containing 10 mM 4-(2-hydroxyethyl)-1-piperazineethanesufonic acid (HBSS−HEPES, pH 7.4) was followed visually over time.

2.6. Cell Viability. The cytotoxicity of the prepare nanoparticles was evaluated by cell proliferation experiments. Briefly, EA.hy926 and U87 cells were seeded in 96-well plates at the density of 1×10^4 cells/well and 1.5×10^4 cells/well, respectively, and allowed to attach overnight. Then, the cell culture medium was replaced by 100 μL of medium containing different concentrations of nanoparticles. After 24 h of incubation, the amount of living cells was determined by the CellTiter Glo luminescence cell viability assay kit (Promega, USA). Each experiment was performed at least in triplicate.

2.7. Cell Uptake of the Nanoparticles. The cell−nanoparticle interactions were studied *in vitro* with hybrid endothelial EA.hy926 and U87 MG brain cells by TEM. About 2 mL/well of 5×10^5 cells/well of EA.hy926 cells or 6×10^5 cells/well of U87 MG cells were seeded in 6-well plates containing 18 × 18 mm coverslip (Menzel-Gläser, Braunschweig, Germany) in each well. After reaching 80% confluency, the medium was replaced by new medium containing 100 μg/mL of each nanoparticle. After 3 h incubation, the nanoparticle suspensions were removed and the cells were washed three times with HBSS (pH 7.4). A 1 mL/well portion of 2.5% glutaraldehyde was added to the cells and incubated at 37 °C for 20 min for cell fixation, followed by washing three times with HBSS. Ultrathin sections of both control and exposed cells to the nanoparticles were prepared as described elsewhere.[24] The TEM images were examined by transmission electron microscopy (Jeol, JEM-1400, Japan) with voltage of 80 kV and magnification between 250× and 10 000×.

2.8. Nanoparticle Plasma Protein Adsorption and Identification. The adsorbed proteins to the nanoparticles' surface were studied as follows. A 200 μg sample of each type of modified nanoparticles was incubated in 1 mL of human plasma at 37 °C for 2 h. After incubation, the nanoparticles were collected by centrifugation and washed twice with Milli-Q water. The proteins were extracted from the plasma treated nanoparticles with sodium dodecyl sulfate polyacrylamide gel electrophoresis (SDS-PAGE). The opsonized nanoparticles (40 μg) were suspended in the PAGE sample buffer (125 mM Tris-HCl pH 6.8, 2% SDS, 5% glycerol, 0.002% bromophenol blue) and incubated at 100 °C for 5 min in order to release and denaturate the adsorbed proteins. The samples were run on a 9% SDS-PAGE-gel for 2 h at a constant voltage of 100 V. The gel was stained with 0.025% Coomassie brilliant blue (Thermo Scientific, USA). The protein bands from sample THCPSi-RGDS were excised alongside with additional protein bands from all the other samples to verify the presence of complement C3 and its derivatives. The excised bands were digested in-gel using sequencing grade modified trypsin (Promega, USA) in 50 mM NH_4HCO_3 buffer (pH 8) at 37 °C overnight.

The peptides obtained from trypsin digestion were separated with liquid chromatography and analyzed with a QSTAR XL hybrid quadrupole time-of-flight mass spectrometer (MS, Applied Biosystems, USA). The proteins were identified from peptide mass fingerprint data with MASCOT search engine (v1.6b25 http://www.matrixscience.com). The mass spectrometer was calibrated with known trypsin autolytic peptides. The MASCOT searches were carried out against the SwissProt database (released 2013_12, http://www.uniprot.org/) which contained 541 954 sequences. Parent ion and fragment mass tolerances were 0.1 and 0.2 Da, respectively. Oxidation of methionine (M) was selected as a variable modification.

DOI: 10.1021/am507827n
ACS Appl. Mater. Interfaces 2015, 7, 2006−2015

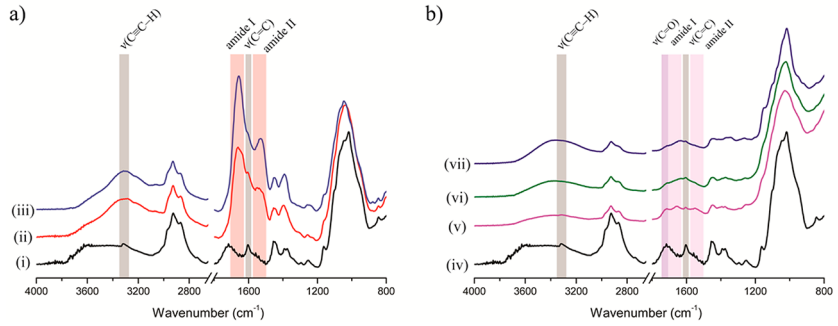

c)

	Mass content (w-%)		
	Carbon	Nitrogen	Hydrogen
THCPSi-alkyne	6.49	0.00	2.198
THCPSi-RGDS	9.32	0.24	2.233
THCPSi-iRGD	10.05	0.52	2.406
THCPSi-PGA	9.92	0.11	2.317
THCPSi-Dex6k	11.16	0.46	2.814
THCPSi-Dex40k	12.79	0.28	3.044

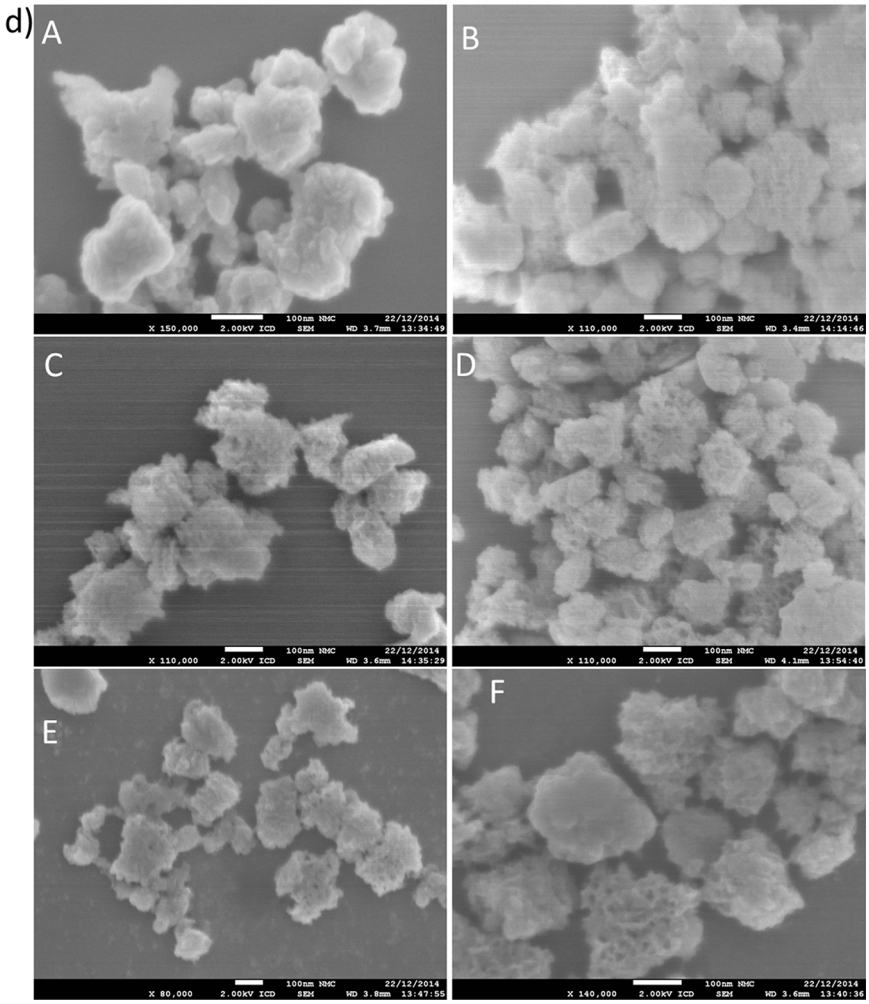

Figure 2. (a and b) FTIR absorbance spectra of THCPSi-alkyne (i and iv), THCPSi-RGDS (ii), THCPSi-iRGD (iii), THCPSi-PGA (v), THCPSi-Dex6k (vi), and THCPSi-Dex40k (vii) nanoparticles. (c) Table of the corresponding elemental contents in each modified nanoparticles determined by elemental analysis. (d) HR-SEM images of the THCPSi-alkyne (A), THCPSi-RGDS (B), THCPSi-iRGD (C), THCPSi-PGA (D), THCPSi-Dex6k (E), and THCPSi-Dex40k (F) nanoparticles. (Scale bar: 100 nm).

DOI: 10.1021/am507827n
ACS Appl. Mater. Interfaces 2015, 7, 2006−2015

Table 1. Hydrodynamic Size, Polydispersity Index (PdI), ζ-Potential, and Conjugation Ratio of the Surface Functionalized THCPSi-Alkyne Nanoparticles

	size (nm)	PdI	ζ-potential (mV)	conjugation ratio[a]
THCPSi-alkyne	176.3 ± 2.6	0.087 ± 0.011	−20.4 ± 0.5	
THCPSi-RGDS	181.6 ± 2.2	0.072 ± 0.003	−22.1 ± 1.0	2.35 ± 1.70
THCPSi-iRGD	186.7 ± 1.1	0.062 ± 0.015	−24.2 ± 0.5	5.83 ± 2.48
THCPSi-PGA	180.9 ± 1.1	0.061 ± 0.015	−31.6 ± 0.2	N.D.[b]
THCPSi-Dex6k	200.5 ± 0.1	0.059 ± 0.020	+22.8 ± 0.3	2.62 ± 0.81
THCPSi-Dex40k	221.9 ± 1.9	0.076 ± 0.004	+14.4 ± 0.6	4.93 ± 1.41

[a]Conjugation ratio presented as the mass percentage of the conjugated biomolecules to the whole modified nanoparticles. [b]TG analysis was inconclusive as the conjugated PGA did not degrade under the experimental conditions tested.

2.9. Statistical Analysis. Results of the quantitative assays were expressed as mean ± s.d. of at least three independent experiments. Student's *t*-test was used to evaluate the significant differences and set at probabilities of $*p < 0.05$ using Origin 8.6 (OriginLab Corp., USA).

3. RESULTS AND DISCUSSION

3.1. Nanoparticle Preparation and Physicochemical Characterization. The THCPSi-alkyne nanoparticles were prepared and characterized as described in the Experimental Procedures section. The nanoparticles presented the following properties: surface area of 176 ± 14 m^2/g, pore volume of 0.53 ± 0.01 cm^3/g, and pore diameter of 12.1 ± 1.2 nm. The functionalized THCPSi-alkyne nanoparticles were prepared via CuAAC (Figure 1). The reaction was carried out at room temperature in mild conditions. The surface conjugation of the nanoparticles was monitored with FTIR (Figure 2a and b). The THCPSi-alkyne shows the successful covalent addition of octadiyne due the presence of a vibration band at 3320 cm^{-1} assigned to the alkyne C≡CH stretching and the ν(C═C) band at 1605 cm^{-1}. After the click reaction, both iRGD and RGDS peptides can be confirmed by the appearance of strong amide I and II vibration bands at 1660 and 1550 cm^{-1}, respectively. After the cycloaddition of PGA to the THCPSi-alkyne, the amide I and II bands of PGA were complemented by the ν(C═O) vibrations of the carboxylic acid side chains appearing as a shoulder to the adjacent amide I band. After the CuAAC reaction with both peptides, PGA and dextrans, the nanoparticles also showed an increase of OH groups on their surfaces, as it can be seen by the presence of a broad OH band above 3100 cm^{-1}. With the THCPSi-Dex6k and THCPSi-Dex40, also the OH scissoring at 1635 cm^{-1} can be observed. Elemental analysis was used to evaluate the content of carbon, nitrogen, and hydrogen of each nanoparticle after surface modification (Figure 2c).[12] After surface modification, the organic components (carbon, nitrogen, and hydrogen) were increased compared to the bare THCPSi-alkyne nanoparticles. Furthermore, the quantitative conjugation ratio of each surface modification was determined by TG analysis (Table 1).

The size and zeta (ζ)-potential of the THCPSi-alkyne nanoparticles with the five surface biofunctionalizing moieties are listed in Table 1. The size of the PSi nanoparticles increased slightly but consistently with the molecular weight (MW) of the conjugated biomolecules. The sizes of the modified nanoparticles were between 170 and 220 nm. All the PSi nanoparticles showed narrow polydispersity (PdI < 0.1). The ζ-potential of the nanoparticles modified with RGDS, iRGD, and PGA remained negative because of the neutral charge of RGDS and iRGD and the negative charge of PGA. For the surface modification of the nanoparticles with dextran 5k Da and dextran 40k Da, the ζ-potential of NPs became positive. The HR-SEM and TEM images showed the size and morphologies of the THCPSi-alkyne nanoparticles after surface modification (Figures 2d and S3). The size of the nanoparticles visualized by HR-SEM and TEM images matched the DLS results. From the HR-SEM and TEM images, we can also observe that the nanoparticles are round-shaped. The surface modification of the THCPSi-alkyne nanoparticles did not significantly change the morphology, shape, and size of the nanoparticles.

Next, the stability of the PSi nanoparticles in high saline solution was evaluated. By surface functionalization, the covalently attached hydrophilic biopolymers onto the surface of the nanoparticles increased extensively the dispersion stability of the nanoparticles in the aqueous buffer solution (Figure 3). Although all the nanoparticles were initially well

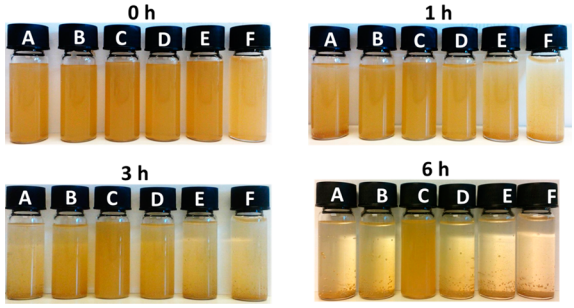

Figure 3. Photographs of the dispersion stability of the nanoparticles: THCPSi-alkyne (A), THCPSi-Dex6k (B), THCPSi-Dex40k (C), THCPSi-PGA (D), THCPSi-RGDS (E), and THCPSi-iRGD (F) at time points 0, 1, 3, and 6 h. For each surface functionalization, 100 μg/mL of the nanoparticles were dispersed in HBSS−HEPES buffer (pH 7.4).

dispersed in HBSS−HEPES buffer using tip-sonication, after 1 h it was visible that the more hydrophobic nanoparticles started to precipitate partially. The stability was monitored up to 6 h, after which THCPSi-Dex40k nanoparticles showed the best stability in HBSS buffer. The aqueous dispersibility and stability of the nanoparticles was time- and surface functionalization-dependent and followed the order: THCPSi-Dex40k > THCPSi-Dex6k ∼ THCPSi-PGA > THCPSi-iRGD > THCPSi-RGDS ∼ THCPSi-alkyne, resembling the order of the MW of the conjugated molecules.

3.2. *In Vitro* Cell Viability. The surface chemistry is one of the main parameters determining the cytocompatibility of nanoparticles. Thus, we next evaluated the *in vitro* viability of endothelial EA.hy926 and brain U87 MG cells incubated with pure THCPSi-alkyne and the surface functionalized nanoparticles using an ATP-based luminescent cell assay (Figure 4).

DOI: 10.1021/am507827n
ACS Appl. Mater. Interfaces 2015, 7, 2006−2015

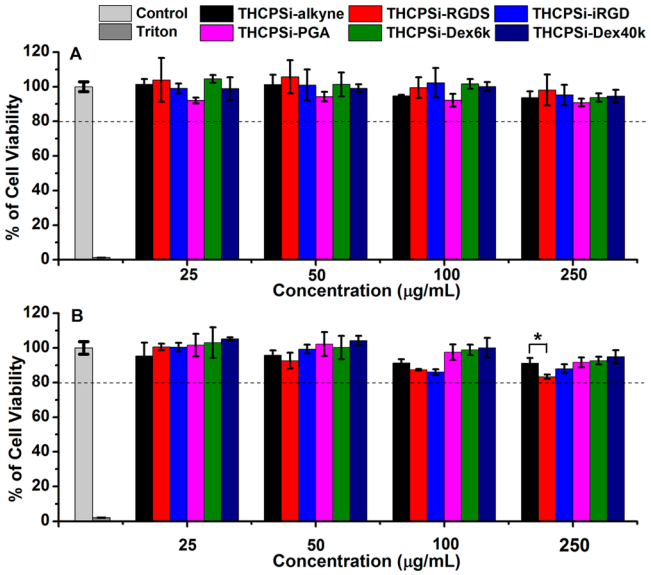

Figure 4. Cell viability of THCPSi-alkyne, THCPSi-RGDS, THCPSi-iRGD, THCPSi-PGA, THCPSi-Dex6k, and THCPSi-Dex40k nanoparticles incubated with EA.hy926 endothelial (A) and brain U87 MG (B) cells for 24 h at 37 °C. The cell viability was determined by an ATP-based CellTiter-Glo luminescence cell viability assay. Error bars represent mean ± s.d. ($n \geq 3$). Dash line indicates the level of 80% cell viability. Cells incubated in cell medium without nanoparticles or treated with cell medium containing 0.1% Triton X-100 were used as positive and negative control, respectively. There was no statistically significant differences on the cell viability between the nanoparticles before and after different surface modifications, except the THCPSi-RGD nanoparticles at a concentration 250 μg/mL ($^*p < 0.05$).

As expected, the results showed that all the nanoparticles had very low toxicity to both EA.hy926 and U87 MG cells with concentrations up to 250 μg/mL. THCPSi nanoparticles have been reported as one type of biomaterials with good biocompatibility.[49] The targeting peptides RGDS and iRGD, and the biodegradable polymers PGA and dextran used in this study are known for the good biocompatibility and widely investigated for biomedical purposes.[19,54−56] With the CuAAC conjugation, the biofunctionalized THCPSi-alkyne nanoparticles presented good cell viability. The studied surface modified nanoparticles are therefore promising candidates for further investigation for biomedical applications that are concerned with low cytotoxicity.

3.3. Cell Uptake of the Surface Functionalized THCPSi-Alkyne Nanoparticles. TEM was used to study the cellular uptake of the prepared nanoparticles (Figure 5). Unmodified THCPSi-alkyne nanoparticles showed very low cell uptake in both EA.hy926 and U87 MG cells, in line with previous cellular studies using this type of THCPSi nanoparticles.[49] RGD can interact with the integrin on the cell's surface, which is widely expressed by both neovascular and tumor cells, and induce integrin $\alpha v\beta 3/5$ mediated cell internalization.[42,57] The TEM images of the intracellular uptake in EA.hy926 cells incubated with THCPSi-RGDS and THCPSi-iRGD nanoparticles showed a significant increase in the nanoparticle cell uptake. The incubation of RGDS- and iRGD-modified nanoparticles with U87 MG cells showed that there were also more nanoparticles localized inside the cytoplasm compared to the bare THCPSi-alkyne nanoparticles. Both modifications showed similar cell uptake efficacy. This is consistent with our previous work of RGDS/iRGD surface functionalization of thermally carbonized PSi nanoparticles.[24]

PGA is a simple polypeptide made from repeating units of a single amino acid namely glutamic acid. The cell−nanoparticle interactions of the PGA-modified THCPSi nanoparticles were also evaluated. The PGA-modified THCPSi nanoparticles showed a slightly higher cell uptake in EA.hy926 cells compared to the bare THCPSi-alkyne nanoparticles but lower than the RGDS- and iRGD-modified THCPSi nanoparticles. Interestingly, PGA-modified THCPSi had very high cell uptake efficacy in U87 MG cells, even more extensive than the RGDS- and iRGD-modified THCPSi nanoparticles. It has been reported that PGA incorporated nanoparticles can undergo γ-glutamyl transpeptidase receptor mediated cell uptake, and thus, enhance the cancer cell uptake.[58] The γ-glutamyl transpeptidase receptor is widely expressed by human neoplasia tissues and cancer cells, including brain carcinoma cell lines.[59] Here, the PGA surface modification induced significant enhanced cell uptake of the nanoparticles in U87 MG cells which might be due to the overexpression of γ-glutamyl transpeptidase receptor on the cell's surface.[60] THCPSi-Dex6k and THCPSi-Dex40k nanoparticles increased the cell uptake in both EA.hy926 and U87 MG cells compared to the bare THCPSi-alkyne nanoparticles. Furthermore, THCPSi-Dex40k nanoparticles showed considerably higher cellular uptake than the THCPSi-Dex6k nanoparticles in both EA.hy926 and U87 MG cells.

The surface functionalization of PSi nanoparticles with targeting peptides can increase the cell uptake of the nanoparticles.[24] Chemical conjugation of dextrans (6 and 40 kDa) to the nanoparticles' surface can enhance the cell−nanoparticle interactions.[61,62] The surface functionalization of the THCPSi-alkyne nanoparticles with both targeting peptide RGD derivatives and polymers (PGA and dextrans) increased the cellular uptake of the nanoparticles in both EA.hy926 and U87 MG cells. In EA.hy926 cells, the intracellular uptake efficacy of the nanoparticles was in the following order: THCPSi-RGDS ~ THCPSi-iRGD > THCPSi-Dex40k > THCPSi-Dex6k > THCPSi-PGA > THCPSi-alkyne. In U87 MG cells, the intracellular uptake efficacy of the nanoparticles was in the following order: THCPSi-PGA > THCPSi-RGDS ~ THCPSi-iRGD > THCPSi-Dex40k > THCPSi-Dex6k > THCPSi-alkyne.

3.4. Plasma Protein Adsorption and Identification. The plasma proteins' association onto the prepared nanoparticles was determined by analyzing the opsonized proteins with SDS-PAGE gel electrophoresis and further verified by mass spectrometry (listed on the right column of the SDS-PAGE photography in Figure 6). THCPSi-Dex40k (Figure 6, **lane G**) showed more negligible protein adsorption for the proteins of MW above 70 kDa, followed by THCPSi-Dex6k (Figure 6, **lane C**), which only adsorbed albumin (MW 69 kDa) in the same range, but the amount of albumin is less than all the other nanoparticles, followed by THCPSi-PGA (Figure 6, **lane F**). THCPSi-alkyne (Figure 6, **lane B**), THCPSi-RGDS (Figure 6, **lane D**), or THCPSi-iRGD (Figure 6, **lane E**) had similar albumin adsorption. Furthermore, only THCPSi-RGDS (Figure 6, **lane D**) and THCPSi-iRGD (Figure 6, **lane E**) nanoparticles adsorbed complementary C3 protein, which is one of the major proteins of immune complement system.[63]

For the proteins of MW 35−70 kDa, the two dextran-modified nanoparticles showed similar protein adsorption profiles, while the other four nanoparticles had similar profiles. The differences of the protein adsorption profiles observed

DOI: 10.1021/am507827n
ACS Appl. Mater. Interfaces 2015, 7, 2006−2015

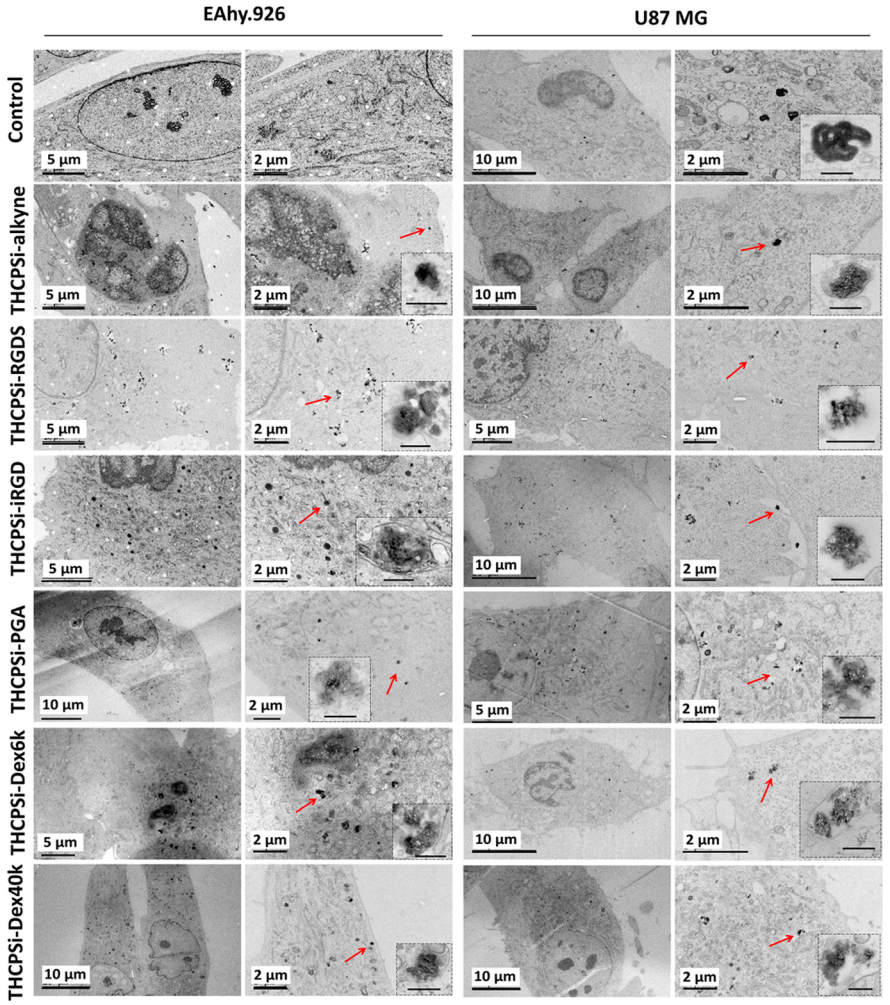

Figure 5. TEM images of the intracellular distribution of the THCPSi-alkyne, THCPSi-RGDS, THCPSi-iRGD, THCPSi-PGA, THCPSi-Dex6k, and THCPSi-Dex40k nanoparticles in EA.hy926 and U87 MG cells. TEM images of ultrathin sections of pure EA.hy926 and U87 MG cells were used as controls or incubated with the different nanoparticles at 37 °C. Inset scale bars are 200 nm. Arrows indicate the samples for each THCPSi nanoparticles.

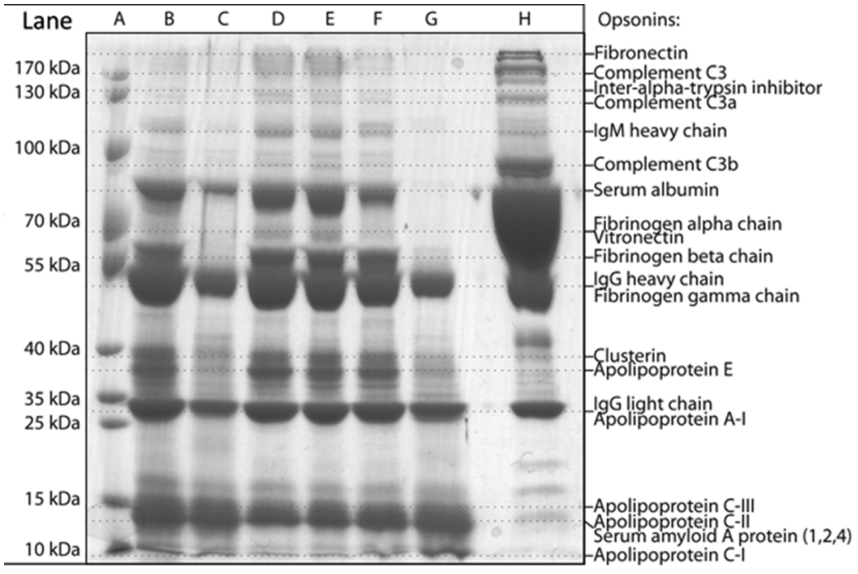

Figure 6. SDS-PAGE separation of the adsorbed plasma proteins on THCPSi-alkyne nanoparticles (lane B), THCPSi-Dex6k (lane C), THCPSi-RGDS (lane D), THCPSi-iRGD (lane E), THCPSi-PGA (lane F), and THCPSi-Dex40k (lane G). Lane A was the MW marker, and lane H was pure human plasma.

DOI: 10.1021/am507827n
ACS Appl. Mater. Interfaces 2015, 7, 2006−2015

between the two groups were that, for the dextran-modified nanoparticles, no fibrinogen β chains adsorption occurred and less adsorption of immunoglobulin G (IgG) heavy chain, fibrinogen γ chain, clusterin, and apolipoprotein E proteins took place. The fibrinogen proteins and immunoglobulins, together with complement proteins, are the major proteins that can active the immune system and uptake the phagocytosis by MPS.[35] In this study, both dextran surface modifications reduced immune proteins (fibrinogen and immunoglobulin G) association onto the nanoparticles, compared to the other surface modification, as well as the bare THCPSi-alkyne nanoparticles. Clusterin is the protein involved, for example, in cell apoptosis, complement mediated cell lysis and membrane recycling.[64] Clusterin has been shown activity as complement inhibitor.[65] Apolipoprotein E is a class of apolipoprotein and has been reported to be involved in the hepatocytic elimination of certain type of nanoparticles.[66] For the plasma proteins with MW below 35 kDa, all the nanoparticles presented a similar protein association profile.

Overall, the THCPSi-Dex40k nanoparticles showed less protein surface adsorption compared to the bare THCPSi-alkyne. Interestingly, it has been reported that positively charged, amino-terminated nanoparticles, had higher protein corona by dynamic light scattering analysis.[67] However, in our study, dextran (6 kDa and 40 kDa) modified THCPSi nanoparticles presented a positive ζ-potential but no evidence of extensive protein association due to the steric repulsion.[40] The PSi nanoparticles after surface modification by targeting peptides and antifouling polymers presented different protein adsorption profiles with the plasma proteins of higher MW ranges. THCPSi-alkyne nanoparticles modified by dextran with higher MW induced less immune proteins adsorption compared to all the other nanoparticles in this study. The mechanism is properly due to the "steric repulsion", which is consistent with other studies reported in the literature.[4,38,68] On the other hand, in terms of peptide-modification, the protein adsorption profiles of RGDS and iRGD modified THCPSi-alkyne nanoparticles were different from the bare THCPSi-alkyne nanoparticles, the polymer PGA or the dextran (both 6k and 40k) modified nanoparticles, which might be due to the different nanoparticle surface chemistry−plasma protein interactions.[69] Both the targeting peptides (RGDS and iRGD) modified PSi nanoparticles did induce complement C3 protein adsorption and convert the C3 protein to C3a/b forms, which are known to active the immune system. Recently, Smith et al. reported that RGD modification of single-walled carbon nanotube significantly enhanced the monocytes-mediated tumor uptake.[70] The plasma proteins association to the nanoparticles can significantly affect the fate of the nanoparticles. However, the mechanism of the effect on the plasma protein opsonization for the *in vivo* fate of targeting peptide-modified nanoparticles is complex due to the possibility of the targeting peptides to specifically interact with the plasma proteins. In terms of cellular uptake, the targeting peptides can significantly enhance the cellular uptake of the nanoparticles. Nevertheless, there is still more work need to be done to correlate the profiles of the plasma protein association with the targeting peptide-modified nanoparticles with the *in vivo* fate of the nanoparticles.

4. CONCLUSIONS

Alkyne-terminated THCPSi nanoparticles with a hydrodynamic size of 170 nm were prepared. Five bioactive hydrophilic molecules, targeting peptides (RGDS and iRGD) and antifouling polymers (PGA and dextran 6 and 40 kDa) were conjugated to the THCPSi-alkyne nanoparticles via the versatile CuAAC click reaction. The stability of the THCPSi-Dex40 nanoparticles in aqueous buffer was significantly increased compared to the bare THCPSi-alkyne nanoparticles. All the THCPSi nanoparticles in this study showed very low cytotoxicity in both EA.hy926 and U87 MG cells. The cell−nanoparticle interactions and cell internalization were enhanced by the surface modification with the aforementioned bioactive molecules. The efficiency of the cell uptake of the modified nanoparticles was cell- and surface chemistry-dependent. Plasma protein adsorption analysis showed that both peptides and polymers modification of the surface of the nanoparticles, as well as the unmodified THCPSi-alkyne, all induced different plasma protein adsorption profiles. The surface modification with dextran 40 kDa to THCPSi-alkyne nanoparticles were more effective in reducing the protein adsorption than the other modification moieties or the unmodified nanoparticles. Both RGDS and iRGD modified nanoparticles presented another pattern of protein adsorption behavior. The plasma protein association "figure-print" of PGA modified THCPSi was more similar (but not the same) with that of the peptides rather than dextran 6k modified nanoparticles. Overall, the alkyne-terminated THCPSi nanoparticles presented highly potential applicability for drug delivery via various surface modifications. The efficient cellular uptake and reducing protein adsorption of THCPSi can be modulated by the surface modification with different moieties to improve the bioactivity and reduce the protein association.

■ ASSOCIATED CONTENT

Supporting Information

More details regarding the NMR and FTIR spectra of the azide-functionalized polymers and the TEM images of all the THCPSi nanoparticles. This material is available free of charge via the Internet at http://pubs.acs.org.

■ AUTHOR INFORMATION

Corresponding Authors

*Tel.: +358-2941-59661. E-mail: helder.santos@helsinki.fi (H.A.S.).

*E-mail: chang-fang.wang@helsinki.fi (C.-F.W.).

Notes

The authors declare no competing financial interest.

■ ACKNOWLEDGMENTS

H.A.S. acknowledges the Academy of Finland (decision numbers 252215 and 256394), the University of Helsinki Research Funds, the Biocentrum Helsinki, and the European Research Council under the European Union's Seventh Framework Programme (FP/2007−2013, grant no. 310892) for financial support. C.-F.W. acknowledges financial support from the Chinese Scholarship Council (grant no. 2009627022).

■ REFERENCES

(1) Zhang, H.; Liu, D.; Shahbazi, M. A.; Mäkilä, E.; Herranz-Blanco, B.; Salonen, J.; Hirvonen, J.; Santos, H. A. Fabrication of a Multifunctional Nano-in-micro Drug Delivery Platform by Microfluidic Templated Encapsulation of Porous Silicon in Polymer Matrix. *Adv. Mater.* **2014**, *16*, 4497−4503.

(2) Xie, J.; Lee, S.; Chen, X. Nanoparticle-Based Theranostic Agents. *Adv. Drug Delivery Rev.* **2010**, *62*, 1064−1079.

DOI: 10.1021/am507827n
ACS Appl. Mater. Interfaces 2015, 7, 2006−2015

(3) Shanmugam, V.; Selvakumar, S.; Yeh, C. S. Near-Infrared Light-Responsive Nanomaterials in Cancer Therapeutics. *Chem. Soc. Rev.* **2014**, *43*, 6254−6287.
(4) Couvreur, P. Nanoparticles in Drug Delivery: Past, Present and Future. *Adv. Drug Delivery Rev.* **2013**, *65*, 21−23.
(5) Sasaki, Y.; Nishina, T.; Yasui, H.; Goto, M.; Muro, K.; Tsuji, A.; Koizumi, W.; Toh, Y.; Takuo, H.; Miyata, Y. Phase II Trial of Nanoparticle Albumin-Bound Paclitaxel as Second-Line Chemotherapy For Unresectable or Recurrent Gastric Cancer. *Cancer Sci.* **2014**, *105*, 812−817.
(6) Rom, J.; Bechstein, S.; Domschke, C.; Golatta, M.; Mayer, C.; Heil, J.; Thum, J.; Smetanay, K.; Windemuth-Kieselbach, C.; Wallwiener, M.; Marme, F.; Schuetz, F.; Sohn, C.; Schneeweiss, A. Efficacy and Toxicity Profile of Pegylated Liposomal Doxorubicin (Caelyx) in Patients With Advanced Breast Cancer. *Anticancer Drugs* **2014**, *25*, 219−224.
(7) Salonen, J.; Laitinen, L.; Kaukonen, A. M.; Tuura, J.; Bjorkqvist, M.; Heikkilä, T.; Vaha-Heikkilä, K.; Hirvonen, J.; Lehto, V. P. Mesoporous Silicon Microparticles For Oral Drug Delivery: Loading and Release of Five Model Drugs. *J. Controlled Release* **2005**, *108*, 362−374.
(8) Santos, H. A.; Bimbo, L. M.; Lehto, V. P.; Airaksinen, A. J.; Salonen, J.; Hirvonen, J. Multifunctional Porous Silicon For Therapeutic Drug Delivery and Imaging. *Curr. Drug Discov. Technol.* **2011**, *8*, 228−249.
(9) Liu, D.; Bimbo, L. M.; Mäkilä, E.; Villanova, F.; Kaasalainen, M.; Herranz-Blanco, B.; Caramella, C. M.; Lehto, V. P.; Salonen, J.; Herzig, K. H.; Hirvonen, J.; Santos, H. A. Co-delivery of a Hydrophobic Small Molecule and a Hydrophilic Peptide by Porous Silicon Nanoparticles. *J. Controlled Release* **2013**, *170*, 268−278.
(10) Sarparanta, M. P.; Bimbo, L. M.; Mäkilä, E. M.; Salonen, J. J.; Laaksonen, P. H.; Helariutta, A. M.; Linder, M. B.; Hirvonen, J. T.; Laaksonen, T. J.; Santos, H. A.; Airaksinen, A. J. The Mucoadhesive and Gastroretentive Properties of Hydrophobin-Coated Porous Silicon Nanoparticle Oral Drug Delivery Systems. *Biomaterials* **2012**, *33*, 3353−3362.
(11) Santos, H. A.; Mäkilä, E.; Airaksinen, A. J.; Bimbo, L. M.; Hirvonen, J. Porous Silicon Nanoparticles For Nanomedicine: Preparation and Biomedical Applications. *Nanomedicine (UK)* **2014**, *9*, 535−554.
(12) Xia, B.; Zhang, W.; Shi, J.; Xiao, S.-J. Engineered Stealth Porous Silicon Nanoparticles via Surface Encapsulation of Bovine Serum Albumin for Prolonging Blood Circulation *in Vivo*. *ACS Appl. Mater. Interface* **2013**, *5*, 11718−11724.
(13) Higashi, G. S.; Becker, R. S.; Chabal, Y. J.; Becker, A. Comparison of Si(111) Surfaces Prepared Using Aqueous Solutions of NH_4F Versus HF. *J. Appl. Phys. Lett.* **1991**, *58*, 1656−1658.
(14) Liu, D.; Mäkilä, E.; Zhang, H.; Herranz, B.; Kaasalainen, M.; Kinnari, P.; Salonen, J.; Hirvonen, J.; Santos, H. A. Nanostructured Porous Silicon-Solid Lipid Nanocomposite: Towards Enhanced Cytocompatibility and Stability, Reduced Cellular Association and Prolonged Drug Release. *Adv. Funct. Mater.* **2013**, *23*, 1893−1902.
(15) James, M.; Ciampi, S.; Darwish, T. A.; Hanley, T. L.; Sylvester, S. O.; Gooding, J. J. Nanoscale Water Condensation on Click-Functionalized Self-Assembled Monolayers. *Langmuir* **2011**, *27*, 10753−10762.
(16) Mäkilä, E.; Bimbo, L. M.; Kaasalainen, M.; Herranz, B.; Airaksinen, A. J.; Heinonen, M.; Kukk, E.; Hirvonen, J.; Santos, H. A.; Salonen, J. Amine Modification of Thermally Carbonized Porous Silicon with Silane Coupling Chemistry. *Langmuir* **2012**, *28*, 14045−14054.
(17) Wu, E. C.; Andrew, J. S.; Cheng, L.; Freeman, W. R.; Pearson, L.; Sailor, M. J. Real-time Monitoring of Sustained Drug Release Using the Optical Properties of Porous Silicon Photonic Crystal Particles. *Biomaterials* **2011**, *32*, 1957−1966.
(18) Boukherroub, R.; Wojtyk, J. T. C.; Wayner, D. D. M.; Lockwood, D. J. Thermal Hydrosilylation of Undecylenic Acid with Porous Silicon. *J. Electrochem. Soc.* **2002**, *149*, H59−H63.
(19) Guan, B.; Ciampi, S.; Le Saux, G.; Gaus, K.; Reece, P. J.; Gooding, J. J. Different Functionalization of the Internal and External Surfaces in Mesoporous Materials for Biosensing Applications Using "Click" Chemistry. *Langmuir* **2011**, *27*, 328−334.
(20) Ciampi, S.; Bocking, T.; Kilian, K. A.; Harper, J. B.; Gooding, J. J. Click Chemistry in Mesoporous Materials: Functionalization of Porous Silicon Rugate Filters. *Langmuir* **2008**, *24*, 5888−5892.
(21) Qin, G.; Santos, C.; Zhang, W.; Li, Y.; Kumar, A.; Erasquin, U. J.; Liu, K.; Muradov, P.; Trautner, B. W.; Cai, C. Biofunctionalization on Alkylated Silicon Substrate Surfaces via "Click" Chemistry. *J. Am. Chem. Soc.* **2010**, *132*, 16432−16441.
(22) Li, Y.; Santos, C. M.; Kumar, A.; Zhao, M.; Lopez, A. I.; Qin, G.; McDermott, A. M.; Cai, C. Click" Immobilization on Alkylated Silicon Substrates: Model for the Study of Surface Bound Antimicrobial Peptides. *Chem.—Eur. J.* **2011**, *17*, 2656−2665.
(23) Li, Y.; Wang, J.; Cai, C. Rapid Grafting of Azido-Labeled Oligo(ethylene glycol)s onto an Alkynyl-Terminated Monolayer on Nonoxidized Silicon via Microwave-Assisted "Click" Reaction. *Langmuir* **2011**, *27*, 2437−2445.
(24) Wang, C. F.; Mäkilä, E. M.; Kaasalainen, M. H.; Liu, D.; Sarparanta, M. P.; Airaksinen, A. J.; Salonen, J. J.; Hirvonen, J. T.; Santos, H. A. Copper-Free Azide-Alkyne Cycloaddition of Targeting Peptides to Porous Silicon Nanoparticles for Intracellular Drug Uptake. *Biomaterials* **2014**, *35*, 1257−1266.
(25) Shahbazi, M. A.; Almeida, P. V.; Mäkilä, E. M.; Kaasalainen, M. H.; Salonen, J. J.; Hirvonen, J. T.; Santos, H. A. Augmented Cellular Trafficking and Endosomal Escape of Porous Silicon Nanoparticles via Zwitterionic Bilayer Polymer Surface Engineering. *Biomaterials* **2014**, *35*, 7488−7500.
(26) Guan, B.; Magenau, A.; Ciampi, S.; Gaus, K.; Reece, P. J.; Gooding, J. J. Antibody Modified Porous Silicon Microparticles for the Selective Capture of Cells. *Bioconjugate Chem.* **2014**, *25*, 1282−1289.
(27) Li, Y.; Cai, C. Click Chemistry-Based Functionalization on Non-Oxidized Silicon Substrates. *Chemistry—Asian J.* **2011**, *6*, 2592−2605.
(28) Kolb, H. C.; Finn, M. G.; Sharpless, K. B. Diverse Chemical Function from a Few Good Reactions. *Angew. Chem., Int. Ed. Engl.* **2001**, *40*, 2004−2021.
(29) Wang, C. F.; Auriola, S.; Hirvonen, J.; Santos, H. A. Conjugation of Peptides to Antisense Interleukin-6 via Click Chemistry. *Curr. Med. Chem.* **2014**, *21*, 1247−1254.
(30) Sapsford, K. E.; Algar, W. R.; Berti, L.; Gemmill, K. B.; Casey, B. J.; Oh, E.; Stewart, M. H.; Medintz, I. L. Functionalizing Nanoparticles with Biological Molecules: Developing Chemistries that Facilitate Nanotechnology. *Chem. Rev.* **2013**, *113*, 1904−2074.
(31) Xi, W.; Scott, T. F.; Kloxin, C. J.; Bowman, C. N. Click Chemistry in Materials Science. *Adv. Funct. Mater.* **2014**, *24*, 2572−2590.
(32) Lallana, E.; Sousa-Herves, A.; Fernandez-Trillo, F.; Riguera, R.; Fernandez-Megia, E. Click Chemistry for Drug Delivery Nanosystems. *Pharm. Res.* **2012**, *29*, 1−34.
(33) Nel, A. E.; Madler, L.; Velegol, D.; Xia, T.; Hoek, E. M.; Somasundaran, P.; Klaessig, F.; Castranova, V.; Thompson, M. Understanding Biophysicochemical Interactions at the Nano-Bio Interface. *Nat. Mater.* **2009**, *8*, 543−557.
(34) Tenzer, S.; Docter, D.; Kuharev, J.; Musyanovych, A.; Fetz, V.; Hecht, R.; Schlenk, F.; Fischer, D.; Kiouptsi, K.; Reinhardt, C.; Landfester, K.; Schild, H.; Maskos, M.; Knauer, S. K.; Stauber, R. H. Rapid Formation of Plasma Protein Corona Critically Affects Nanoparticle Pathophysiology. *Nat. Nanotechnol.* **2013**, *8*, 772−81.
(35) Liu, D.; Liu, F.; Song, Y. K. Recognition and Clearance of Liposomes Containing Phosphatidylserine are Mediated By Serum Opsonin. *Biochim. Biophys. Acta* **1995**, *12*, 140−146.
(36) Hu, Y.; Xie, J.; Tong, Y. W.; Wang, C.-H. Effect of PEG Conformation and Particle Size on the Cellular Uptake Efficiency of Nanoparticles with the HepG2 Cells. *J. Controlled Release* **2007**, *118*, 7−17.
(37) Dai, Q.; Walkey, C.; Chan, W. C. W. Polyethylene Glycol Backfilling Mitigates the Negative Impact of the Protein Corona on

DOI: 10.1021/am507827n
ACS Appl. Mater. Interfaces 2015, 7, 2006−2015

Nanoparticle Cell Targeting. *Angew. Chem., Int. Ed. Engl.* **2014**, *53*, 5093−5096.
(38) Pozzi, D.; Colapicchioni, V.; Caracciolo, G.; Piovesana, S.; Capriotti, A. L.; Palchetti, S.; De Grossi, S.; Riccioli, A.; Amenitsch, H.; Lagana, A. Effect of Polyethyleneglycol (PEG) Chain Length on the Bio-Nano-Interactions Between PEGylated Lipid Nanoparticles and Biological Fluids: From Nanostructure to Uptake in Cancer Cells. *Nanoscale* **2014**, *6*, 2782−2792.
(39) Sacchetti, C.; Motamedchaboki, K.; Magrini, A.; Palmieri, G.; Mattei, M.; Bernardini, S.; Rosato, N.; Bottini, N.; Bottini, M. Surface Polyethylene Glycol Conformation Influences the Protein Corona of Polyethylene Glycol-Modified Single-Walled Carbon Nanotubes: Potential Implications on Biological Performance. *ACS Nano* **2013**, *7*, 1974−1989.
(40) Vauthier, C.; Persson, B.; Lindner, P.; Cabane, B. Protein Adsorption and Complement Activation for Di-Block Copolymer Nanoparticles. *Biomaterials* **2011**, *32*, 1646−1656.
(41) Li, B.; Wang, Q.; Wang, X.; Wang, C.; Jiang, X. Preparation, Drug Release and Cellular Uptake of Doxorubicin-Loaded Dextran-b-Poly(Varepsilon-Caprolactone) Nanoparticles. *Carbohydr. Polym.* **2013**, *93*, 430−437.
(42) Sugahara, K. N.; Teesalu, T.; Karmali, P. P.; Kotamraju, V. R.; Agemy, L.; Girard, O. M.; Hanahan, D.; Mattrey, R. F.; Ruoslahti, E. Tissue-Penetrating Delivery of Compounds and Nanoparticles Into Tumors. *Cancer Cell* **2009**, *16*, 510−520.
(43) Monopoli, M. P.; Aberg, C.; Salvati, A.; Dawson, K. A. Biomolecular Coronas Provide the Biological Identity of Nanosized Materials. *Nat. Nanotechnol.* **2012**, *7*, 779−786.
(44) Bonduelle, C.; Huang, J.; Ibarboure, E.; Heise, A.; Lecommandoux, S. Synthesis and Self-Assembly of ″Tree-Like″ Amphiphilic Glycopolypeptides. *Chem. Commun.* **2012**, *48*, 8353−8355.
(45) Marguet, M.; Bonduelle, C.; Lecommandoux, S. Multicompartmentalized Polymeric Systems: Towards Biomimetic Cellular Structure and Function. *Chem. Soc. Rev.* **2013**, *42*, 512−529.
(46) Huang, J.; Bonduelle, C.; Thevenot, J.; Lecommandoux, S.; Heise, A. Biologically Active Polymersomes From Amphiphilic Glycopeptides. *J. Am. Chem. Soc.* **2012**, *134*, 119−122.
(47) Goñi-de-Cerio, F.; Mariani, V.; Cohen, D.; Madi, L.; Thevenot, J.; Oliveira, H.; Uboldi, C.; Giudetti, G.; Coradeghini, R.; Garanger, E.; Rossi, F.; Portugal-Cohen, M.; Oron, M.; Korenstein, R.; Lecommandoux, S.; Ponti, J.; Suárez-Merino, B.; Heredia, P. Biocompatibility Study of Two Diblock Copolymeric Nanoparticles for Biomedical Applications by *In Vitro* Toxicity Testing. J. *Nanopart. Res.* **2013**, *15*, 1−17.
(48) Peng, S. F.; Yang, M. J.; Su, C. J.; Chen, H. L.; Lee, P. W.; Wei, M. C.; Sung, H. W. Effects of Incorporation of Poly(Gamma-Glutamic Acid) in Chitosan/DNA Complex Nanoparticles on Cellular Uptake and Transfection Efficiency. *Biomaterials* **2009**, *30*, 1797−808.
(49) Bimbo, L. M.; Sarparanta, M.; Santos, H. A.; Airaksinen, A. J.; Mäkilä, E.; Laaksonen, T.; Peltonen, L.; Lehto, V. P.; Hirvonen, J.; Salonen, J. Biocompatibility of Thermally Hydrocarbonized Porous Silicon Nanoparticles and Their Biodistribution in Rats. *ACS Nano* **2010**, *4*, 3023−3032.
(50) Kovalainen, M.; Mönkäre, J.; Mäkilä, E.; Salonen, J.; Lehto, V. P.; Herzig, K. H.; Jarvinen, K. Mesoporous Silicon (PSi) for Sustained Peptide Delivery: Effect of PSi Microparticle Surface Chemistry on Peptide YY3−36 Release. *Pharm. Res.* **2012**, *29*, 837−846.
(51) Schatz, C.; Louguet, S.; Le Meins, J.-F.; Lecommandoux, S. Polysaccharide-block-polypeptide Copolymer Vesicles: Towards Synthetic Viral Capsids. *Angew. Chem., Int. Ed. Engl.* **2009**, *48*, 2572−2575.
(52) Sanson, C.; Schatz, C.; Le Meins, J. F.; Brulet, A.; Soum, A.; Lecommandoux, S. Biocompatible and Biodegradable Poly-(Trimethylene Carbonate)-b-Poly(L-Glutamic Acid) Polymersomes: Size Control and Stability. *Langmuir* **2010**, *26*, 2751−2760.
(53) Fagerlund, G. Determination of Specific Surface by the BET Method. *Mater. Constr.* **1973**, *6*, 239−245.
(54) Estevanato, L. L.; Lacava, L. M.; Carvalho, L. C.; Azevedo, R. B.; Silva, O.; Pelegrini, F.; Bao, S. N.; Morais, P. C.; Lacava, Z. G. Long-Term Biodistribution and Biocompatibility Investigation of Dextran-Coated Magnetite Nanoparticle Using Mice as the Animal Model. *J. Biomed. Nanotechnol.* **2012**, *8*, 301−308.
(55) Shen, J.; Meng, Q.; Sui, H.; Yin, Q.; Zhang, Z.; Yu, H.; Li, Y. iRGD Conjugated TPGS Mediates Codelivery of Paclitaxel and Survivin shRNA for the Reversal of Lung Cancer Resistance. *Mol. Pharmacol.* **2013**, *11*, 2579−2591.
(56) Dobrovolskaia, M. A.; Aggarwal, P.; Hall, J. B.; McNeil, S. E. Preclinical Studies To Understand Nanoparticle Interaction with the Immune System and Its Potential Effects on Nanoparticle Biodistribution. *Mol. Pharmaceutics* **2008**, *5*, 487−495.
(57) Ruoslahti, E. Peptides as Targeting Elements and Tissue Penetration Devices for Nanoparticles. *Adv. Mater.* **2012**, *24*, 3747−3756.
(58) Peng, S.-F.; Tseng, M. T.; Ho, Y.-C.; Wei, M.-C.; Liao, Z.-X.; Sung, H.-W. Mechanisms of Cellular Uptake and Intracellular Trafficking with Chitosan/DNA/Poly(γ-Glutamic Acid) Complexes as a Gene Delivery Vector. *Biomaterials* **2011**, *32*, 239−248.
(59) Pompella, A.; De Tata, V.; Paolicchi, A.; Zunino, F. Expression of Gamma-Glutamyltransferase in Cancer Cells and its Significance in Drug Resistance. *Biochem. Pharmacol.* **2006**, *71*, 231−238.
(60) Cornford, E. M.; Cornford, M. E. New Systems for Delivery of Drugs to the Brain in Neurological Disease. *Lancet Neurol.* **2002**, *1*, 306−315.
(61) Liu, P.; Yue, C.; Sheng, Z.; Gao, G.; Li, M.; Yi, H.; Zheng, C.; Wang, B.; Cai, L. New Systems for Delivery of Drugs to the Brain in Neurological Disease. *Polym. Chem. (UK)* **2014**, *5*, 874−881.
(62) Filipović, N.; Stevanović, M.; Nunić, J.; Cundrič, S.; Filipič, M.; Uskoković, D. Synthesis of Poly(Varepsilon-Caprolactone) Nanospheres in the Presence of the Protective Agent Poly(Glutamic Acid) and their Cytotoxicity, Genotoxicity and Ability to Induce Oxidative Stress in HepG2 Cells. *Colloids Surf. B Biointerfaces* **2014**, *117*, 414−424.
(63) Sim, R. B.; Laich, A. Serine Proteases of the Complement System. *Biochem. Soc. Trans.* **2000**, *28*, 545−550.
(64) Jones, S. E.; Jomary, C. Clusterin. *Int. J. Biochem. Cell Biol.* **2002**, *34*, 427−431.
(65) Tschopp, J.; Chonn, A.; Hertig, S.; French, L. E. Clusterin, the Human Apolipoprotein and Complement Inhibitor, Binds to Complement C7, C8 Beta, and the B Domain of C9. *J. Immunol.* **1993**, *151*, 2159−2165.
(66) Yan, X.; Kuipers, F.; Havekes, L. M.; Havinga, R.; Dontje, B.; Poelstra, K.; Scherphof, G. L.; Kamps, J. A. The role of Apolipoprotein E in the Elimination of Liposomes from Blood by Hepatocytes in the Mouse. *Biochem. Biophys. Res. Commun.* **2005**, *328*, 57−62.
(67) Moyano, D. F.; Saha, K.; Prakash, G.; Yan, B.; Kong, H.; Yazdani, M.; Rotello, V. M. Fabrication of Corona-Free Nanoparticles with Tunable Hydrophobicity. *ACS Nano* **2014**, *8*, 6748−6755.
(68) D'Addio, S. M.; Saad, W.; Ansell, S. M.; Squiers, J. J.; Adamson, D. H.; Herrera-Alonso, M.; Wohl, A. R.; Hoye, T. R.; Macosko, C. W.; Mayer, L. D.; Vauthier, C.; Prud'homme, R. K. Effects of Block Copolymer Properties on Nanocarrier Protection from In Vivo Clearance. *J. Controlled Release* **2012**, *162*, 208−217.
(69) Mahon, E.; Salvati, A.; Baldelli Bombelli, F.; Lynch, I.; Dawson, K. A. Designing the Nanoparticle-Biomolecule Interface for ″Targeting and Therapeutic Delivery″. *J. Controlled Release* **2012**, *161*, 164−174.
(70) Smith, B. R.; Ghosn, E. E.; Rallapalli, H.; Prescher, J. A.; Larson, T.; Herzenberg, L. A.; Gambhir, S. S. Selective Uptake of Single-Walled Carbon Nanotubes by Circulating Monocytes for Enhanced Tumour Delivery. *Nat. Nanotechnol.* **2014**, *9*, 481−487.

DOI: 10.1021/am507827n
ACS Appl. Mater. Interfaces 2015, 7, 2006−2015